



PERGAMON

Available online at [www.sciencedirect.com](http://www.sciencedirect.com)

SCIENCE @ DIRECT®

Polyhedron 22 (2003) 1377–1383



POLYHEDRON

[www.elsevier.com/locate/poly](http://www.elsevier.com/locate/poly)

# Isotope effects in the V(IV)-malate complex formation system

Yong-Hong Zhang, Yasutoshi Ban, Masao Nomura, Yasuhiko Fujii\*

*Research Laboratory for Nuclear Reactors, Tokyo Institute of Technology, O-okayama, Meguro-ku, Tokyo 152-8550, Japan*

Received 19 November 2002; accepted 19 February 2003

## Abstract

Cation-exchange displacement chromatography of  $\text{VO}^{2+}$  was carried out for studying vanadium isotope fractionation in the malate complex formation system. After the chromatographic elution, the heavier isotope  $^{51}\text{V}$  was found to be enriched at the front boundary of the  $\text{VO}^{2+}$  band, which indicates that the heavier isotope is preferentially fractionated into the malate complex in the aqueous solution phase. The isotope separation coefficient  $\varepsilon$  ( $=\alpha-1$ ) for  $^{50}\text{V}$  and  $^{51}\text{V}$  was obtained as  $1.0 \times 10^{-4}$  for the malate system at 298 K. This value is smaller than the ones for  $\text{UO}_2^{2+}$  and  $\text{Cu}^{2+}$  in the same ligand systems. Binuclear complex species in  $\text{UO}_2^{2+}$  and  $\text{Cu}^{2+}$  solutions may be attributed to the larger isotope effects in the complex formation system. Through comparison of the reported separation coefficient values of  $\varepsilon$  per unit mass differences ( $\varepsilon/\Delta M$ ) of the alkali, alkaline earth and transition elements in the complex formation systems, it is suggested that the stronger the complex of the concerned element, the more the isotopic fractionation can obtain.

© 2003 Elsevier Science Ltd. All rights reserved.

**Keywords:** Isotopic fractionation; Ion-exchange chromatography; Complex formation; Dimerization; Separation coefficient; Molecular vibration

## 1. Introduction

Vanadium has been receiving increasing attention in geochemistry and biology, because this element is an essential trace element [1]. Naturally occurring vanadium consists of two stable isotopes with the mass numbers 50 and 51, of which the isotope  $^{50}\text{V}$  is a weakly radioactive isotope with the half-life of  $1.4 \times 10^{17}$  years. It has been well known that vanadium is highly accumulated in some petroleum and the blood of certain invertebrates, and isotopic fractionations, i.e., deviations in the  $^{50}\text{V}/^{51}\text{V}$  isotopic ratio, were observed in these organic materials [2,3]. Because transition metals participate actively in multiple biologic and low-temperature inorganic chemical reactions, their isotopic variability offers an unexplored potential as biogeochemical and geochemical tracers [4–7]. The main phenomena leading to isotopic fractionations involve isotope exchange reactions and kinetic processes of

isotopomers; the former gives equilibrium isotope effects and the latter gives the kinetic isotope effects. Isotopomers or molecules containing different isotopes of an element that display slight differences in their vibrational frequencies due to the differences in the zero-point energies, with the result that equilibrium processes in which they are involved display isotopic fractionation [8]. So far, the physico-chemical studies on vanadium isotope effects have been very limited. Laboratory experiments on vanadium isotope effects in equilibrium exchange reactions would assist the elucidation of the isotope fractionation in nature and in biological processes. In the present work, the vanadium isotope effects are studied by using ion-exchange chromatography.

Mass fractionation on ion-exchange resins has been extensively studied by chromatographic processes of isotopes of many elements involving alkali, alkaline earth and transition metals [9–14]. The observation for most elements follows the conventional quantum mechanical effect due to molecular vibration theory established by Bigeleisen and Mayer in 1947 [15], i.e., the heavier isotope is preferable to be fractionated into the strongly bound chemical species. From the previous IR spectroscopic and chromatographic studies on the uranium isotope effect in the formation of uranyl

\* Corresponding author. Tel.: +81-3-5734-2378; fax: +81-3-5734-2958.

E-mail addresses: [yhzhang@nr.titech.ac.jp](mailto:yhzhang@nr.titech.ac.jp) (Y.-H. Zhang), [yfujii@nr.titech.ac.jp](mailto:yfujii@nr.titech.ac.jp) (Y. Fujii).

complexes, it was found that the lighter isotope  $^{235}\text{U}$  is enriched in the uranyl ( $\text{UO}_2^{2+}$ ) carboxylate complexes and the isotope separation coefficients  $\epsilon$  of the uranyl complex systems are linearly proportional to the shift of the asymmetric stretching vibration  $\nu_3$  of  $\text{O}=\text{U}=\text{O}$  in uranyl complexes, which reflects the reduction of the  $\text{O}=\text{U}=\text{O}$  bond strength by complex formation [16–18]. The results indicated that the lighter isotope  $^{235}\text{U}$  is enriched in the strongly coordinated species. The larger the stability constant of the complex, the more is the  $^{235}\text{U}$  enriched in the complex. Among some selected uranyl carboxylate complexes, the malate ligand has shown the largest separation coefficient. For this reason, malate was applied to the investigation of the isotopic fractionation of copper [11] and vanadium in the present work.

Tetravalent vanadium, the most stable oxyocations existing in the form of the entity  $\text{VO}^{2+}$ , is very similar to the uranyl ion  $\text{UO}_2^{2+}$  and can form a wide variety of stable complexes [19], especially with hydroxycarboxylate function groups. In the present work, malate was selected as a ligand to measure the isotopic fractionation of vanadium in a complex formation system by cation-exchange chromatography. Discussion is also extended to the reported isotope effects in complex formation systems of alkali, alkaline earth and transition elements in order to demonstrate stronger complex formation of the elements that may cause larger isotope effects. It is hoped that more insight will be gained into the origin of the isotope effect and understanding the theory of isotope effects.

## 2. Experimental

### 2.1. Chromatographic processes

The chromatography system used in the present study consists of two Pyrex columns (1.0 cm i.d. and 100 cm long) and a high-pressure pump (controlling the flow rate of the feeding solution), connected in series with a 0.8 mm Teflon tube. The temperature was set at 298 K throughout the experiment by circulating thermostated water through the jackets of the column. A fraction collector was used to collect the effluent in small fractions.

The columns were packed with strongly acidic cation-exchange resin SQS-6, highly porous, small diameter of 70–90  $\mu\text{m}$ , developed by Asahi Chemical Industry. At the beginning of the chromatographic operation, the resin packed in the column was conditioned by elution with 2 M HCl solution to remove the impurities and convert it completely into  $\text{H}^+$  form, and washed thoroughly with redistilled water. A measured volume of the 0.2 mol  $\text{dm}^{-3}$   $\text{VOSO}_4 + 0.1$  mol  $\text{dm}^{-3}$   $\text{H}_2\text{SO}_4$  solution was fed into the column to form the  $\text{VO}^{2+}$  adsorption band, which is visible, dark cyan, in contrast

to the orange yellow resin in  $\text{H}^+$  form. The length of the band was 30 cm. The  $\text{VO}^{2+}$  band was then eluted through the  $\text{H}^+$  form resin bed at the flow rate of 6.0  $\text{cm}^3 \text{h}^{-1}$  with 0.1 mol  $\text{dm}^{-3}$  solution of ammonium malate, prepared from DL-malic acid ( $\text{COOH}-\text{CH}_2\text{CHOH}-\text{COOH}$ ) and  $\text{NH}_3 \cdot \text{H}_2\text{O}$  (Wako, analytical-reagent grade), and adjusted to pH 7.5. The band velocity was approximately 1.0  $\text{cm h}^{-1}$ . After migration (the migration length was 2 m, the total eluent volume used was 1180 ml), the effluent was collected in small fractions, and then submitted to the analyses of the pH, vanadium concentration and the isotopic abundance ratio.

### 2.2. Chemical and isotopic analysis

The vanadium concentration in each fraction was measured with an inductively coupled plasma atomic emission spectrometer (ICP-AES, Model SPS 1500VR, Seiko Instruments), at the most sensitive line of 309.311 nm. Wavelength adjustment and sensitivity calibration were performed before measurement. The pH of the effluent fraction was measured by a pH meter with a glass electrode.

The determination of vanadium isotope ratios  $^{50}\text{V}/^{51}\text{V}$  was carried out using a single-focusing 23 cm radius,  $90^\circ$  magnetic sector field, Finnigan MAT 261 mass spectrometer, equipped with a thermal-ionization ion source and an Faraday cup collector for detection of the  $\text{V}^+$  ion currents. The filament unit, which generates the  $\text{V}^+$  ions, comprises two rhenium ribbon filaments, one for evaporation and the other for ionization.

Before applying the mass analyses, each sample was first pretreated with concentrated  $\text{HNO}_3$  and heated to dryness to decompose the organic materials, and then converted into the form of chloride by the addition of concentrated HCl. A portion of each sample containing 20–30  $\mu\text{g}$  vanadium was loaded onto the center of the evaporation filament homogeneously and thermally ionized by the ionization filament.

It should be noted that the mass scanning over the range 50–52 was always made to rigorously correct the isobaric interference by  $^{50}\text{Cr}$ , because chromium (involving isotopes of mass number 50) is contained in the rhenium filaments. The interference of  $^{50}\text{Ti}$  was found to be negligible. The  $^{50}\text{Cr}$  peak height was calculated by multiplying the measured peak height of  $^{52}\text{Cr}$  with the natural abundance ratio of  $^{50}\text{Cr}$  and  $^{52}\text{Cr}$ .

The mass scanning over the range 50–52 was repeated about 48 times for 1 h. The vanadium isotopic ratio of the sample was calculated by averaging all the height ratios of the recorded peaks of  $^{50}\text{V}$  and  $^{51}\text{V}$ . The total time for the mass spectrometric measurement of one sample was approximately 2.5 h.

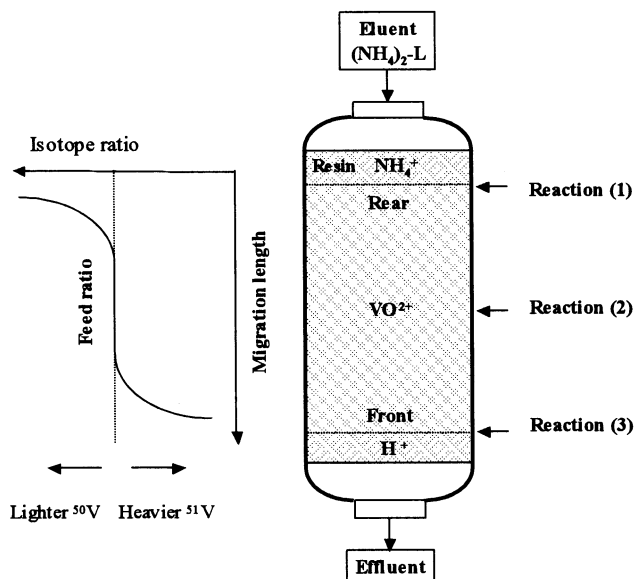


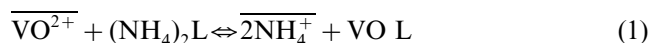
Fig. 1. The mechanism of vanadium isotope separation by cation-exchange chromatography.

### 3. Results

The mechanism of vanadium isotope separation by cation-exchange chromatography was illustrated in Fig. 1. Chromatography was conducted in a band displacement manner. The reactions involved in the band chromatographic system are presented in terms of the general expression for the reactions as follows, by

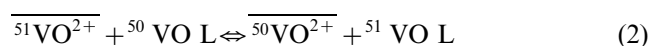
abbreviating malic acid as  $H_2L$  and the malate ion as  $L^{2-}$ .

At the leading boundary of the vanadium band, the adsorbed vanadyl ions are released from the resin forming complexes with the ligand supplied by the eluent.



where bars denote the resin phase.

During the elution developing through the vanadyl band, the isotope exchange reaction (2) takes place repeatedly between vanadyl–carboxylate complexes in the external solution phase and the vanadyl ions in the resin phase.



The separation factor  $\alpha$ , is defined in the present system as:

$$\alpha = \frac{[{}^{50}V/{}^{51}V]_r}{[{}^{50}V/{}^{51}V]_s} = 1 + \varepsilon \quad (3)$$

where the brackets denote the abundance ratio of given isotopes, the subscripts r and s represent the resin and solution phases, respectively.

When the vanadyl–carboxylate complex species reach the leading boundary of the band, the vanadyl complexes were dissociated, and the free vanadyl ion is readsorbed into the resin phase.

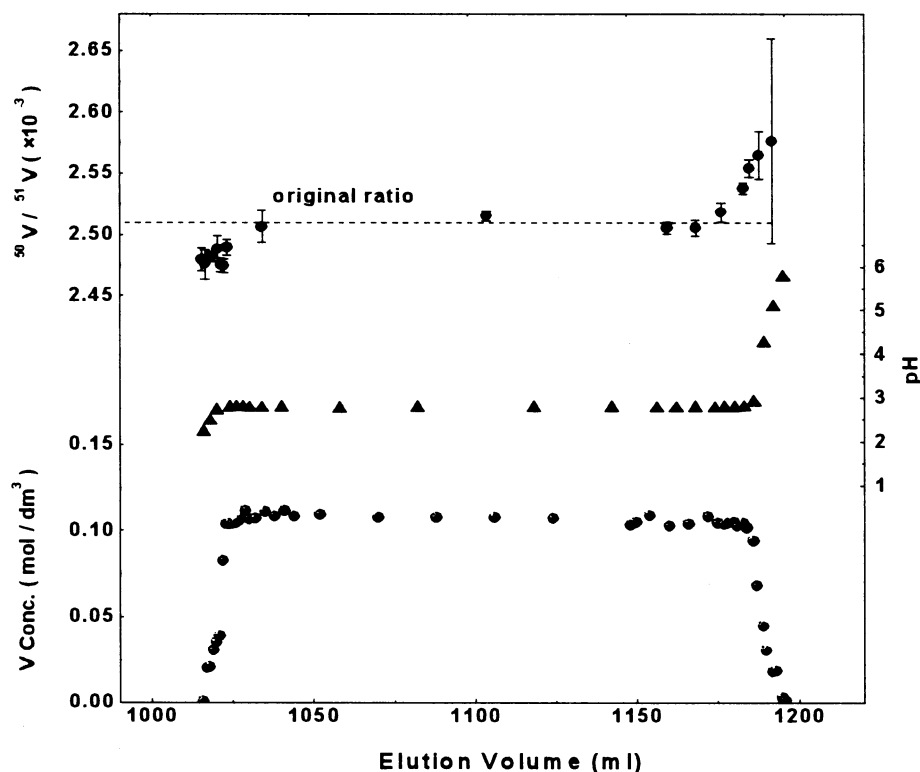
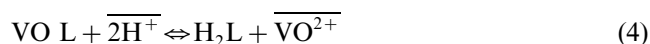


Fig. 2. Chromatogram and measured isotopic ratios in the vanadyl malate system.

The results obtained by the above-stated chemical and isotopic analyses are plotted in Fig. 2. The profile of  $\text{VO}^{2+}$  concentration in the effluent fraction corresponds to  $\text{VO}^{2+}$  band in the column. The chromatography is found to be conducted in an almost ideal displacement manner with sharp band boundaries at both edges of the band. Since, the stability constant of vanadyl malate complex species is larger than that of ammonium malate [20] and the total selectivity of the cation-exchange resin for divalent vanadyl ions is larger than that for protons, the reactions (1) and (4) at leading and trailing boundaries tend to proceed to the right sides and make sharp boundaries at both edges of the band. The sharp band boundaries are also featured in the pH change.

It is obvious from the profile of isotopic ratios in the malate system illustrated in Fig. 2 that the heavier isotope  $^{51}\text{V}$  is enriched at the leading edge and the lighter isotope  $^{50}\text{V}$  enriched at the trailing edge, i.e., the isotope exchange reaction represented by reaction (2) concentrated the heavier isotope  $^{51}\text{V}$  in aqueous solution. The results are interpreted by the mechanism that the heavier isotope  $^{51}\text{V}$  is preferentially fractionated into the vanadyl malate complex species in an aqueous solution and moves down at a relatively faster velocity to the leading edge, while the lighter isotope  $^{50}\text{V}$  is preferentially retained in the vanadyl ions in the resin and eluted down at a lower velocity, resulting in the accumulation at the trailing edge. The results suggest that the equilibrium constant of reaction (2) should be larger than unity. This is consistent with the prediction that the heavier isotope is expected to fractionate into the strongly bound chemical species based on the theory of isotope effects in molecular vibration.

We generally use the term of the separation coefficient  $\varepsilon$  ( $=\alpha - 1$ ) to express the isotope fractionation, which is calculated from the experimental data using the isotopic enrichment curves of the front or rear boundary according to the equation developed by Spedding et al. [21], and Kakihana and Kanzaki [22] (see Appendix A).

In this work, the  $\varepsilon$  value was calculated as  $1.0 \times 10^{-4}$  by using the data of the isotope  $^{50}\text{V}$  enrichment zone (rear part of the chromatogram).

#### 4. Discussion

In the present work, the concentration of vanadium in the plateau region of the chromatogram is approximately  $0.1 \text{ mol cm}^{-3}$ , which is in agreement with the concentration of malate ligand in the feed eluent. This fact indicates that the vanadyl malate complex is produced according to reaction (1). The eluent in the adsorption band region shows the pH value of 2.78 in Fig. 2.

Table 1  
Separation coefficients  $\varepsilon$  of malate and  $\text{EDTA}^{4-}$  complex systems by cation-exchange chromatography

Metal ion	Isotope pair measured	Complex formation system	$T$ (K)	Separation coefficient, $\varepsilon$ ( $\times 10^{-4}$ )	$\varepsilon/\Delta M$ ( $\times 10^{-4}$ )	pH in plateau region of chromatogram	Dominant complex formation	Reference
$\text{VO}^{2+}$	50/51	malate	298	1.0	1.0	2.8	monomer	present work
$\text{Cu}^{2+}$	63/65	malate	312	2.8	1.4	3.5–4	dimer	[11]
		$\text{EDTA}^{4-}$	323	0.13	0.065	2.5–3	monomer	[14]
$\text{Gd}^{3+}$	158/160	malate	312	0.092	0.045	4.5–5	monomer	[10]
		$\text{EDTA}^{4-}$	332	0.25	0.125	2–2.5	monomer	[10]
$\text{UO}_2^{2+}$	235/238	malate	298	2.2	0.73	2–2.5	dimer	[17]
		$\text{EDTA}^{4-}$	298	0.6	0.2	2–5	monomer	[23]

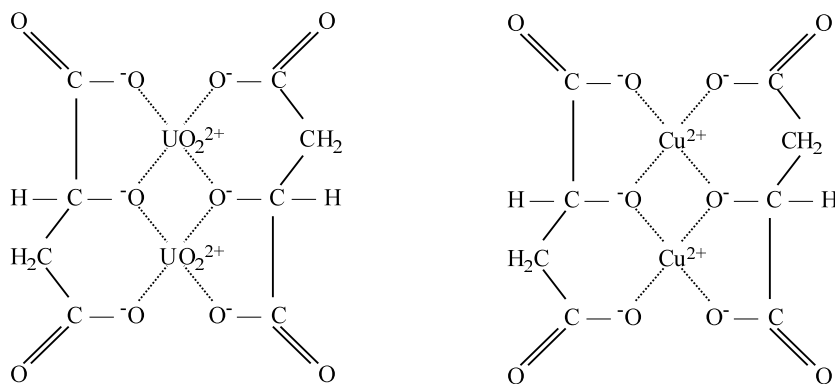


Fig. 3. The possible binuclear chelate structures of Cu(II)–malate and U(VI)–malate complexes.

Table 1 presents the separation coefficient  $\varepsilon$  and the related data of the vanadyl malate system observed in this work by cation-exchange displacement chromatography, along with the results reported from the  $\text{UO}_2^{2+}$ ,  $\text{Gd}^{3+}$  and  $\text{Cu}^{2+}$  in malate and  $\text{EDTA}^{4-}$  ligand exchange systems.

Malic acid forms a wide variety of complex species with multivalent metal ions and usually acts as a bidentate ligand through the hydroxyl and the  $\alpha$ -carboxyl oxygen atoms [24]. In the pH range 2–4, the vanadyl malate complex has been reported to exist in the form of the mononuclear 1:1 complex [20]. The gadolinium malate complex in the chromatogram of  $\text{Gd}^{3+}$  in previous work is also a mononuclear complex [25]. In contrast to  $\text{VO}^{2+}$  and  $\text{Gd}^{3+}$ ,  $\text{Cu}^{2+}$  or  $\text{UO}_2^{2+}$  ions predominantly exist in the form of binuclear complexes,  $\text{Cu}_2\text{L}_2$  and  $(\text{UO}_2)_2\text{L}_2$ , in the pH range 2–4 [26] [27]. The interaction of malic acid with  $\text{Cu}^{2+}$  or  $\text{UO}_2^{2+}$  results in the occurrence of a dimerization reaction of malate chelates in the pH range 2–4, where the  $\alpha$ -hydroxyl group of the malate ligand is involved in the bridging; the possible structures of these two binuclear chelates of  $\text{Cu}^{2+}$  and  $\text{UO}_2^{2+}$  are illustrated in Fig. 3. In addition, it is reported that the binuclear complex is more stable than the mononuclear, which explains its presence at lower pH values.

Recently, Maréchal and Albarède [28] reported that the Zn isotopic fractionation factor is smaller than the Cu isotopic fractionation in the HCl complex system by elution chromatography. They discussed that the large isotope effect of copper is probably due to the presence of polynuclear molecules of the chloride complex ( $\text{Cu}_2\text{Cl}_6^{2-}$ ), where Cu is occupying two different sites in the compound. This discussion may be applicable to the values of  $\varepsilon$  in Table 1 which is indicating the results obtained for malate and  $\text{EDTA}^{4-}$  complexes.  $\text{EDTA}^{4-}$  was expected to make more strong coordination bonds with  $\text{Cu}^{2+}$  than malate. However,  $\varepsilon$  of Cu–EDTA is smaller than that of Cu–malate. On the other hand, the separation coefficient of Gd–EDTA is larger than that

of the Gd–malate system due to the stronger complex formation with  $\text{EDTA}^{4-}$  than malate. This is reasonable since mononuclear complexes of  $\text{Gd}^{3+}$  exist in acidic solutions in both  $\text{EDTA}^{4-}$  and malate systems [25]. The existence of a binuclear in  $\text{UO}_2$ –malate complex may also be the reason for the much larger separation coefficient value than that of  $\text{EDTA}^{4-}$  systems, in which no polymer nuclear complex is formed.

Theoretically,  $\varepsilon$  is proportional to  $\Delta M$  and inversely proportional to square of both the atomic weight  $M$  and absolute temperature  $T$  [14]:

$$\varepsilon \propto \Delta M / M^2 T^2 \quad (5)$$

This means that the log–log plots of the values of  $\varepsilon$  per unit mass differences ( $\varepsilon/\Delta M$ ) versus atomic weight are expressed by a line with a slope of  $-2$  when the complex conditions are similar among the considered elements. In Fig. 4, reported separation coefficients  $\varepsilon$  of other alkali, alkaline earth and transition elements in ligand exchange reactions are also plotted. Taking a panoramic view of isotope fractionation in complex formation systems observed by displacement chromatography using strongly acidic cation-exchange resin plotted in Fig. 4, it is seen that alkali and alkaline earth elements approximately fall on the straight line with the slope of  $-2$ , while most  $\varepsilon$ 's of the transition elements plotted are located at higher places than the line for alkali and alkaline earth elements. This is probably due to the strong complex formation of the transition elements.

The Cu–malate system shows a relatively large value of  $\varepsilon$  compared with other systems of complex formation. In addition, it is noted that U(VI)–malate shows an irregularly large value of  $\varepsilon$  when Eq. (5) is considered.

In general, the isotope effects or the isotope separation coefficient depends on temperature and the dependency is expressed by Eq. (5). Concerning the U(VI)–malate system, Ismail et al. [29] studied the temperature dependence of  $\varepsilon$  and found that  $\varepsilon$  is increased with temperature in the experimental range from 288 to 343



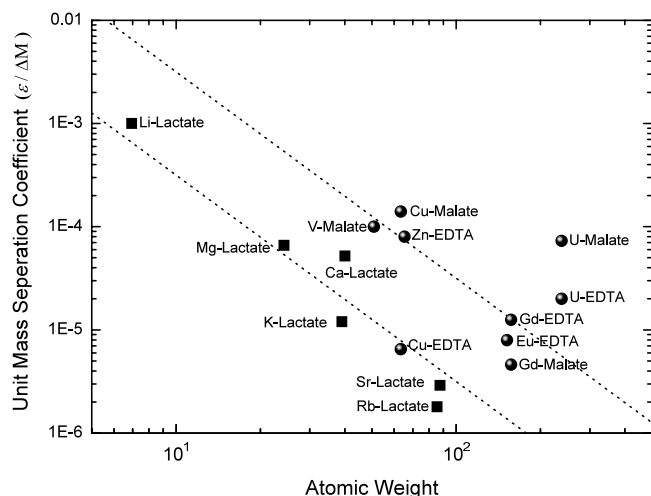


Fig. 4. Isotope effects in ligand exchange reactions observed by cation-exchange chromatography (■: alkali and alkaline earth group metals, ●: transition group metals. Li, Mg, Ca, K, Sr and Rb are taken from Refs. [9]; Cu [11,14], Zn [13], Eu [12], Gd [10], U [17,23]).

K. The value of  $\varepsilon$  in the U(VI)–malate system was shown to be expressed by

$$\varepsilon = A/T^2 + B/T \quad (6)$$

where  $A$  and  $B$  are constant with opposite signs. This pattern of the temperature dependence is very similar to one which was seen in the U(IV)–U(VI) exchange system [30]. The isotope effects in U(IV)–U(VI) exchange has been explained by the term of nuclear field shift, which has been introduced into the chemical isotope effects by Bigeleisen [31].

The temperature dependence of  $\varepsilon$  in the vanadium malate system has not been studied so far. The results obtained in the present work are indicating the features of normal isotope effects based on the classical theory of molecular vibration.

## 5. Conclusion

Isotope fractionations between the vanadyl malate complex in aqueous solution and vanadyl ions in cation-exchange resin were experimentally observed by ion-exchange displacement chromatography. The heavier isotope  $^{51}\text{V}$  was enriched in the species in the aqueous solution phase at the front boundary of the vanadyl ion adsorption band, while the lighter isotope  $^{50}\text{V}$  was enriched in the species in the resin phase at the rear boundary. The separation coefficient of the  $^{50}\text{V}/^{51}\text{V}$  isotopic pair was obtained as  $1.0 \times 10^{-4}$  for the malate system. The  $\varepsilon/\Delta M$  value of  $\text{VO}_2^{2+}$  was expected to be much larger than the  $\varepsilon/\Delta M$  values of  $\text{Gd}^{3+}$  and  $\text{UO}_2^{2+}$  in the malate system due to the smaller atomic weight of V than those of Gd and U. In the present work, the  $\varepsilon/\Delta M$

value of  $\text{VO}_2^{2+}$  was found to be much larger than that of Gd; however it was not so much larger than  $\text{UO}_2^{2+}$ . Also, the  $\varepsilon/\Delta M$  value of  $\text{VO}_2^{2+}$  is found to be smaller than that of  $\text{Cu}^{2+}$  in the malate system. Dimerization in  $\text{UO}_2^{2+}$  and  $\text{Cu}^{2+}$  complexes may affect their isotope effects.

## Acknowledgements

We are very grateful to Professor Y. Ikeda and Dr. M. Harada of Tokyo Institute of Technology (TIT) for their kind cooperation in the ICP–AES measurement.

## Appendix A: Calculation of separation coefficient $\varepsilon$

Separation coefficient  $\varepsilon$  in ion-exchange displacement chromatography is calculated in term of following equation:

$$\varepsilon = \sum C_i |R_i - R_o| / QR_o(1 - R_o) \quad (7)$$

where subscript  $i$  indicates the sample fraction number,  $o$  the original feed,  $C$  the total amount of isotopes,  $Q$  the total exchange capacity of the resin and  $R$  the isotope atom fraction. The larger the deviation of the value  $\varepsilon$  from zero, the greater is the isotope effect. The summation of the equation is taken for the enriched zone or for the depleted one. These summations yield the same value of  $\varepsilon$ , because of the mass balance between the front and the rear of the band.

## References

- [1] N.D. Chasteen, Vanadium in Biological Systems, Kluwer Academic Publishers, Dordrecht, 1990.
- [2] G.D. Flesch, J. Capellen, H.J. Svec, Adv. Mass Spectrom. 3 (1966) 571.
- [3] P.I. Premović, I.R. Tonsa, L. López, M.S. Pavlović, O.M. Nešković, S. LoMonaco, D.M. Dorđević, M.V. Veljković, J. Inorg. Biochem. 80 (2000) 153.
- [4] B.L. Beard, C.M. Johnson, L. Cox, H. Sun, K.H. Nealson, C. Aguilar, Science 285 (1999) 1889.
- [5] C.N. Maréchal, P. Télouk, C. Douchet, F. Albarède, Geochim. Geophys. Geosyst. 1 (2000) (Paper No. 1999.GC000029).
- [6] X.K. Zhu, R.K. O’Nions, Y. Guo, N.S. Belshaw, D. Rickard, Chem. Geol. 163 (2000) 139.
- [7] X.K. Zhu, R.K. O’Nions, Y. Guo, B.C. Reynolds, Science 287 (2000) 2000.
- [8] H.C. Urey, L.J. Grieff, J. Am. Chem. Soc. 57 (1935) 321.
- [9] T. Oi, H. Kakihana, in: Y. Fujii, T. Ishida, H. Takeuchi (Eds.), Bull. Tokyo Inst. Technol., Special issue 1, 1992, pp. 343. ISSN 0387-6144.
- [10] J. Chen, M. Nomura, Y. Fujii, F. Kawakami, M. Okamoto, J. Nucl. Sci. Technol. 29 (1992) 1086.
- [11] M.A. Matin, M. Nomura, Y. Fujii, J.R. Chen, Sep. Sci. Technol. 33 (1998) 1075.
- [12] I.M. Ismail, M. Nomura, Y. Fujii, J. Chromatogr., A 808 (1998) 185.

- [13] Y. Ban, M. Aida, M. Nomura, Y. Fujii, *J. Ion Exchange (Jpn. Assoc. Ion Exchange)* 13 (2002) 46.
- [14] I.M. Ismail, M.A. Matin, M. Nomura, S. Begum, M. Aida, Y. Fujii, *J. Ion Exchange (Jpn. Assoc. Ion Exchange)* 13 (2002) 40.
- [15] J. Bigeleisen, M.G. Mayer, *J. Chem. Phys.* 15 (1947) 261.
- [16] Y. Tanaka, J. Fukuda, M. Okamoto, M. Maeda, *J. Inorg. Nucl. Chem.* 43 (1981) 3291.
- [17] H.Y. Kim, M. Kakihana, M. Aida, K. Kogure, M. Nomura, Y. Fujii, M. Okamoto, *J. Chem. Phys.* 81 (1984) 6266.
- [18] S.P. McGlynn, J.K. Smith, W.C. Neely, *J. Chem. Phys.* 35 (1961) 105.
- [19] J. Selbin, *Chem. Rev.* 65 (1965) 153.
- [20] M. Helena, S.F. Teixeira, J.C. Pessoa, L.F.V. Boas, *Polyhedron* 11 (1992) 697.
- [21] F.H. Spedding, J.E. Powell, H.J. Svec, *J. Am. Chem. Soc.* 77 (1955) 6125.
- [22] H. Kakihana, T. Kanzaki, *Bull. Tokyo Inst. Technol. (Tokyo Inst. Technol.)* 90 (1969) 77.
- [23] A.C. Rutenberg, J.S. Drury, *J. Inorg. Nucl. Chem.* 31 (1969) 2289.
- [24] J.D. Pedrosa de Jesus, in: G. Wilkinson, R.D. Gillard, J.A. McCleverty (Eds.), *Comprehensive Coordination Chemistry*, vol. 2, Pergamon Press, Oxford, 1987, pp. 461–486.
- [25] N.K. Davidenko, *Russ. J. Inorg. Chem.* 9 (1964) 859.
- [26] K.S. Rajan, A.E. Martell, *J. Inorg. Nucl. Chem.* 29 (1967) 463.
- [27] K.S. Rajan, A.E. Martell, *J. Inorg. Nucl. Chem.* 26 (1964) 1927.
- [28] C. Maréchal, F. Albarède, *Geochim. Cosmochim. Acta* 66 (2002) 1499.
- [29] I.M. Ismail, M. Nomura, M. Aida, Y. Fujii, *Z. Naturforsch., A* 57 (2002) 247.
- [30] M. Nomura, N. Higuchi, Y. Fujii, *J. Am. Chem. Soc.* 118 (1996) 9127.
- [31] J. Bigeleisen, *J. Am. Chem. Soc.* 118 (1996) 3676.